Control of Two-wheels Inverted Pendulum Mobile Robot Using Full Order Sliding Mode Control

Nawawi S.W, Ahmad M.N, Osman J.H.S

Faculty of Electrical Engineering,
University Technology Malaysia,
81310, Skudai, Johor Bahru, Malaysia
Contact: sophan@fke.utm.my

Abstract

The research on two-wheel inverted pendulum or commonly call balancing robot has gained momentum over the last decade in a number of robotic laboratories around the world This paper deals with the modeling of 2-wheels Inverted Pendulum and the design of Full Order Sliding Mode Control (FOSMC) for the system. The mathematical model of 2-wheels inverted pendulum system that is highly nonlinear is derived. The final model is then represented in state-space form and the system suffers from mismatched condition. A robust controller based on Sliding Mode Control is proposed to perform the robust stabilization and disturbance rejection of the system. A computer simulation study is carried out to access the performance of the proposed control law.

***Keywords*:**
Two-wheels inverted pendulum, sliding mode control, mismatched condition.

1. Introduction

Wheeled inverse pendulum model have evoked a lot of interest recently and at least one commercial product (Segway) is available [1],[2],[3],[4],[5]. The robot in this consideration has two independent driving wheels in same axis, and the gyro type sensor to know the inclination angular velocity of the body and rotary encoders to know wheels rotation. Due to its configuration with two coaxial wheels, each wheel is coupled to a geared dc motor. The vehicle is able to do stationary U-turns while keeping balance it pole. Such vehicles are of interest because they have a small foot-print and can turn on dime. The kinematics model of the system has been proved to be uncontrollable and therefore balancing of the pendulum is only achieved by considering dynamic effects [6]. Such robots are characterized by the ability to balance on two wheels and spin on the spot. This additional maneuverability allows easy navigation on various terrains, turn sharp corners and traverse small steps or curbs. These capabilities have the potential to solve a number of challenges in industries and society. For example, a motorized wheelchair utilizing this technology would give the operator greater maneuverability and thus access to places most able-body people take for granted. Small cart built utilizing this technology allows humans to travel short distances in a small area or factories area as proposed to using car or buggies which is more polluting [4].

In this work, a mathematical model of 3 degree-of-freedom (DOF) 2-wheels inverted pendulum is derived and the model will be used for the design of a new robust controller. The dynamic modeling is done directly in terms of variables which are of interest with respect to the planning and control of the 2-wheeled inverted pendulum position, inclination, speed and open for further exploration on heading orientation. A Newtonian approach is used to derive the equations [5]. The state space equation of the system is in the following form:

$$\dot{\mathbf{X}}(t) = \mathbf{A}\mathbf{X}(t) + \mathbf{B}\mathbf{X}(t) + \mathbf{f}(\mathbf{X}, t)$$

where **A** and **B** are constant matrices and **f** (**X** ,*t*) is the uncertainty matrix. The uncertainty matrix contains the components of the chassis and both wheels disturbance of the system. The deterministic approach is used to get the bounded condition value of the model for controller design purpose. Simulation result of pole placement controller versus PISMC controller is shown. Result for both controllers is discussed.

2.0 Dynamic Model

Modeling is the process of identifying the principal physical dynamic effects to be considered in analyzing a system, writing the differential and algebraic equations from the conservative laws and property laws of the

relevant discipline, and reducing the equations to a convenient differential equation model [10]. In order to develop the control system, mathematical model is established to predict the behavior before applied into real system. Actually, the dynamics refer to a situation, which is varying with time [10]. The dynamic performance of a balancing robot depends on the efficiency of the control algorithms and the dynamic model of the system. This plant mathematical model only consider for time invariant. By using Kane's method three motion equation is obtain. The coordinate system for the robot is described in Figure 2.

$$3(m_c+m_s)\ddot{x}-m_s d\cos\phi\ddot{\phi}+m_s d\sin\phi(\dot{\phi}^2+\dot{\psi}^2)=-\left(\frac{\alpha_3+\beta_3}{R}\right)$$

(1)

$$\left[(3L^2+\frac{1}{2R^2})m_c+m_s d^2\sin^2\phi+I_2\right]\ddot{\psi}+m_s d^2\sin\phi\dot{\psi}\dot{\phi}=\frac{L}{R}(\alpha_3-\beta_3)$$

(2)

$$m_s d\cos\phi\ddot{x}+(-m_s d^2-I_3)\ddot{\phi}+m_s d^2\sin\phi\cos\phi\dot{\phi}^2+m_s gd\sin\phi=\alpha_3+\beta_3$$
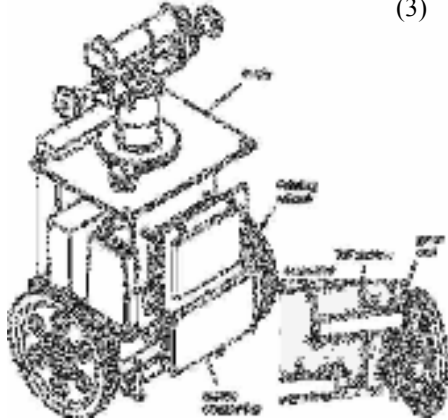
(3)

Figure 1: Two-wheeled Inverted Pendulum robot by Kim et. al [6]
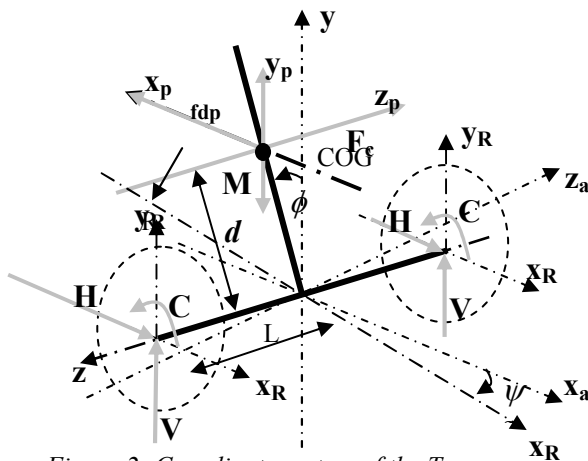

Figure 2: Coordinate system of the Two-wheeled Inverted Pendulum

The **non-linear state space form** is derive from motion equation is given by:

$$\begin{bmatrix}\dot{x}\\\ddot{x}\\\dot{\phi}\\\ddot{\phi}\\\dot{\psi}\\\ddot{\psi}\end{bmatrix}=\begin{bmatrix}0&1&0&0&0&0\\0&0&0&A_{24}&0&A_{26}\\0&0&0&1&0&0\\0&0&0&A_{44}&0&A_{46}\\0&0&0&0&0&1\\0&0&0&0&0&A_{66}\end{bmatrix}\begin{bmatrix}x\\\dot{x}\\\phi\\\dot{\phi}\\\psi\\\dot{\psi}\end{bmatrix}+\begin{bmatrix}0&0\\B_{21}&B_{22}\\0&0\\B_{41}&B_{42}\\0&0\\B_{61}&B_{62}\end{bmatrix}\begin{bmatrix}\alpha_3\\\beta_3\end{bmatrix}+\begin{bmatrix}0\\F_2\\0\\F_4\\0\\0\end{bmatrix}$$

(note: details in appendices)

(4)

3. 0 Controller Design

The theoretical dynamic model is applied to govern the entire system to construct the control system. The dynamic model in equation (4) is a nonlinear model. It should be linearized in the way to design a linear controller. At zero of tilt angle, the robot system has its quasi-equilibrium state. So in this case the linearized model is assumed that the variation of the tilt angle is small enough to neglected. Then we have this linearized model in state space form. Parameter being used is d=0.1m, I_2=3.679x10^{-3} kgm^2, I_3=28.07x10^{-3} kgm^2, m_s=4.315kg, L=0.1m, R=0.073m, m_c=0.503kg. (m_s is mass of body and m_c mass of wheel).

Linear model in state space form:

$$\begin{bmatrix}\dot{x}\\\ddot{x}\\\dot{\phi}\\\ddot{\phi}\\\dot{\psi}\\\ddot{\psi}\end{bmatrix}=\begin{bmatrix}0&1&0&0&0&0\\0&0&A_{23L}&0&0&0\\0&0&0&1&0&0\\0&0&A_{43L}&0&0&0\\0&0&0&0&1&0\\0&0&0&0&0&0\end{bmatrix}\begin{bmatrix}x\\\dot{x}\\\phi\\\dot{\phi}\\\psi\\\dot{\psi}\end{bmatrix}+\begin{bmatrix}0&0\\B_{21L}&B_{22L}\\0&0\\B_{41L}&B_{42L}\\0&0\\B_{61L}&B_{62L}\end{bmatrix}\begin{bmatrix}\alpha_3\\\beta_3\end{bmatrix}$$

(note: details in appendices)

(5)

After conducting the linearization and the test of controllability and observability, the overall control scheme is develop. As shown in Figure 3, the tilt sensor, gyroscope and digital encoder measured six variables. All variables is feedback to the controller. The controller computes the state variables and produces the control input to stabilize and navigate the robot by multiplying the feedback gains and the value of the feedback variables subtract the reference values. The computed voltage is then decoupled and modified to the actual voltage to be applied to the right and left drive wheels [6].
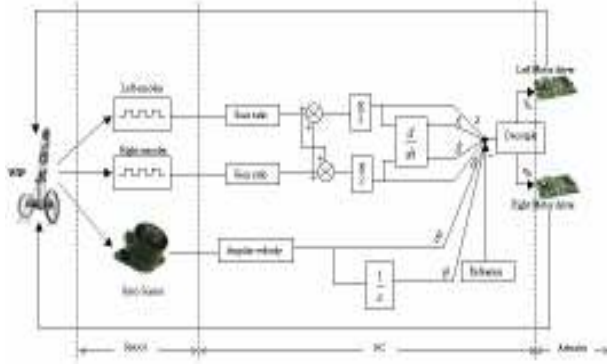
Figure 3: WIP Control chart

3.1 LQR controller

Linear Quadratic Regulator Controller is based on state-feedback control principle. The control gain u=-Kx is obtained base on the performance index J and the solution of the matrix Riccati equation is used as follow:

$$J = \int_0^t x^T Qx + u^T Ru)dt \qquad (7)$$

$$K = R^{-1}B^T P \qquad (8)$$

$$-\dot{P} = A^T P + PA + Q - PBR^{-1}B^T P \qquad (9)$$

Where Q and R should be selected. Usually a simple guideline is to choose these matrices to be diagonal and make the diagonal entry positive large for any variable need to be small in the time domain [11]. In two wheeled inverted pendulum robot, the most important variable to control is tilt angle, ϕ. Therefore the value of Q is firstly set and then R the identity matrix is set. More weight is given to diagonal term for ϕ for good performance. For small rising time and low overshoot for the overall control, Q is tuned to be as equation (10) through several simulations. After getting good value of Q, the feedback gain K is obtained as equation (11). The result of simulation is shown in Figure 7, Figure 8 and Figure 9.

$$Q = \begin{bmatrix} 200 & 0 & 0 & 0 & 0 & 0 \\ 0 & 5 & 0 & 0 & 0 & 0 \\ 0 & 0 & 19.3 & 0 & 0 & 0 \\ 0 & 0 & 0 & 1 & 0 & 0 \\ 0 & 0 & 0 & 0 & 1 & 0 \\ 0 & 0 & 0 & 0 & 0 & 0.05 \end{bmatrix} \quad \begin{matrix}(10)\\ \textbf{3.2}\end{matrix}$$

$$K = \begin{bmatrix} 1.1672 & 2.0932 & 0.0859 & 0.1129 & 35.163 & 9.1 \\ 0.1343 & 0.2119 & -0.1760 & -0.1934 & 10.315 & 2.67 \end{bmatrix}$$

FOSMC Controller Design

The typical structure of a sliding mode controller (SMC) is composed of a nominal part and additional terms to deal with model uncertainty. The way SMC deals with uncertainty is to drive the plants state trajectory onto a sliding surface and maintain the error trajectory on this surface for all subsequent times. The advantage of SMC is that the controlled system becomes insensitive to system disturbances. For the nonlinear model in equation (2.6), by using deterministic method the nominal values of matrices A and B is calculated. Let the dynamic model of the system take the following state space form:

$$\dot{x} = Ax + Bu + f(x) \qquad (3.1)$$

Note that $f(x)$ is stick to original form represent a nonlinear function describing the deviation from linearity in term of disturbances and un-modeled dynamic.

The sliding surface is defined such that the state tracking error converges to zero with input reference. Conventional sliding mode approach defines the sliding surface as $\sigma[x(t)] = Cx(t)$, where C is a vector of known coefficients to be designed base on the linear model of the system. The coefficients in the vector C completely determine the sliding surface. Full Order sliding surface has been proposed in [8],[9],[10],[11], to improve the tracking performance and disturbance rejection properties of conventional sliding mode approach. The PI sliding surface is defines as follows:

$$\sigma[x(t)] = Cx(t) - \int_0^t (CA - CBK)x(\tau)d\tau \qquad (3.2)$$

Where, $C \in \Re^{mxn}$ and $K \in \Re^{mxn}$ are constant matrices. The matrix K satisfies $\lambda(A + BK) < 0$ and C is chosen so that CB is non singular. The control objective now turns to find a control law to drive $\sigma[x(t)]$ towards zero based on the state space model in equation (3.1). By defining a Lyapunov function:

$$V(\sigma) = \frac{1}{2}[\sigma]^2 \qquad (3.3)$$

It can be guaranteed that the sliding surface $\sigma[x(t)] = 0$ is reached in finite time by choosing equation (3.4) to ensure that $\dot{V} = \sigma\dot{\sigma} \le 0$.

$$\dot{\sigma} = -\eta^2 \, \mathrm{sgn}(\sigma) \qquad (3.4)$$

Where, η is tunable parameter. Taking the derivative of PI sliding surface in equation (3.2), the following equation is obtained.

$$\dot{\sigma} = C\dot{x} - [CA + CBK]x \qquad (3.6)$$

By substituting equation (3.1) and (3.4) into (3.6) and with some mathematical manipulations in term u, equivalent control equation (3.7) is obtained.

$$u_{eq} = Kx - (CB)^{-1}Cf - (CB)^{-1}\eta^2 sign\sigma \qquad (3.7)$$

Then by using same poles with the pole-placement control method, to maintain the desired specifications, the value of K is obtain easily using matlab. And the tunable parameter η=100 is used. Finally the parameter of matrices C=[7899 5400 20 200 77 500;81 1 600 91 150 13] is tune by heuristic to get the superior performances. The result of simulation is shown in Figure 7, Figure 8 and Figure 9.

3.2.1 Stability Analysis.

The Lyapunov's method of stability analysis is in principle the most general method for determination of stability for nonlinear or time varying system. This concept is introduced by Russian mathematician A.M Lyapunov.

This section will determine the stability for the dynamics of the system during sliding mode.

$$\dot{x}(t) = M\,x(t) \quad :\text{where: } M = A+BK \quad (3.8)$$

The system of equation (3.8) is said to be stable if every eigenvalue of M has a negative real part. This can be shown if and only if for any given positive definite symmetric matrix Q, the Lyapunov equation:

$$M^T P + PM = -Q \qquad (3.9)$$

has a unique symmetric solution P and P is positive definite. Let the Lyapunov function candidate for the system is chosen as

$$V(t) = x(t)^T Px(t) \qquad (3.10)$$

where $x(t)$ represents the solution of equation 3.8 and P is the solution of the matrix Lyapunov equation such as equation (3.9). Differentiating equation 3.10 with respect to time, t gives

$$\dot{V}(t) = \dot{x}(t)Px(t) + x(t)^T P\dot{x}(t)$$
$$= [Mx(t)]^T Px(t) + x(t)^T P[Mx(t)]$$
$$= x(t)^T M^T Px(t) + x(t)^T PMx(t)$$
$$= x(t)^T [M^T P + PM]x(t)$$
$$= -x(t)^T Qx(t)$$

Since the derivative of the Lyapunov function, $V(t)$ is negative, the system is said to be absolutely stable during sliding mode.
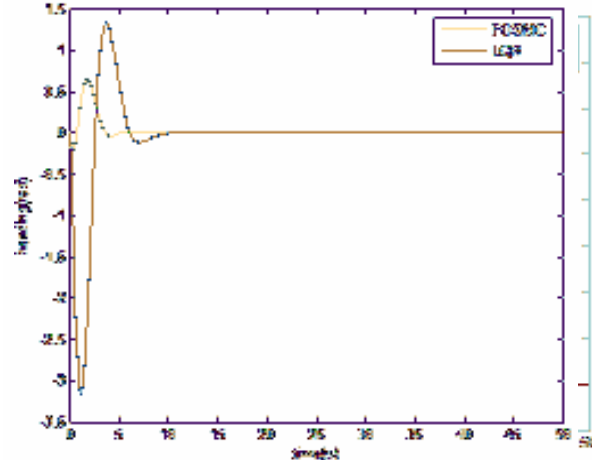
4.0 Simulation Result and Discussion

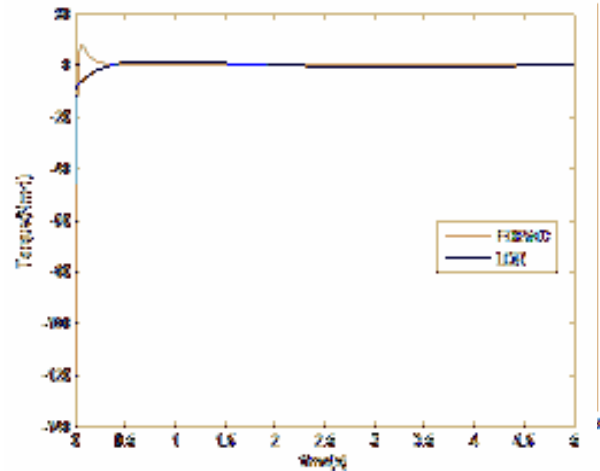Figure 7: Heading control of two-wheeled inverted pendulum

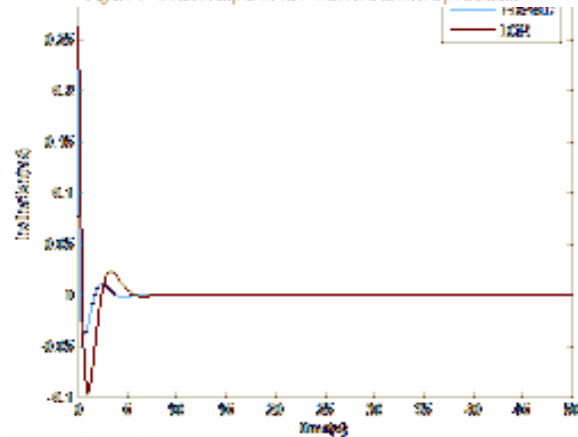Figure 8 Control Input of two-wheeled inverted pendulum

Figure 9 Inclination response of two-wheeled inverted pendulum

The upright balancing is the most fundamental control for two-wheeled inverted pendulum robot because no other control is possible without stable upright balancing. Maintaining the robot's upright balancing is similar to controlling a common inverted pendulum. However, the structure of the two-wheeled inverted pendulum robot is not identical to that of the widely known inverted pendulum.

For instance, in a typical inverted pendulum, the inverted rod or body is connected to the base with a bearing that allows free rotational between the base and upper pendulum however there is no bearing between the base and the upper body of the two wheeled inverted pendulum robot. Nonetheless both cases of the two-wheeled inverted pendulum robot more or less similar because, when no external force or torque is applied, the wheel turns around and the axle and the upper body falls on the floor. When the upright balancing is occur, this operation is consider for more stable operation. The robot should stay in the same position. The upright balancing enables the robot to keep its original position without losing its balance. In the initial condition, the robot was tilted at 15° but the angular velocity of the tilt angle was zero. In this paper the result of speed of robot is not shown.

As can be seen in figure 4 to figure 8, the tilt angle of the mass center of the robot cross the horizontal axis were within 8 second for LQR controller and less then 5 second for FOSMC controller. However, more than 6 second lapsed for position of the center of the robot to return to the original position. It happens for both controllers. But FOSMC gives a good response in heading control in term of overshoot and settling time. Although there is a slightly high value input torque for the FOSMC compare to LQR. This will be effect to implementation into the real hardware. But it's possible if there are good actuators or input control circuit to drive the torque to be at rational values for implementation. Finally it can be seen, the result are satisfactory and upright balancing was successful.

5.0 Conclusion
In this paper a two-wheeled inverted pendulum type robot is discussed. It has the advantage of mobility from without caster and an innate clumsy motion for balancing. To analyze this robot mechanism, Newtonian method of 3-DOF modeling is used to conduct an exact type of dynamic modeling. The simulation result is successfully shown that FOSMC has a good

response to achieve the desired characteristic compare to LQR. With some modification of hardware and software, this work can be carried out for experimental purpose to verify the simulation result. And lastly the 3-DOF dynamical modeling, along with simulation analysis on the two-wheeled inverted pendulum robot should expedite the introduction of this kind of robot in daily life.

References
[1] Salerno, A. and Angeles, J., "Nonlinear Controllability of Quasiholonomic Mobile Robot". Proc. IEEE ICRA, Taiwan, 2003.
[2] Salerno, A. and Angeles, J.,"The control of semi-autonomous two-wheeled robot undergoing large payload variations". Proc. IEEE ICRA, New Orleans, April 2004, pp. 1740-1745.
[3] Ha, Y.S. and Yuta, S.,"Trajectory tracking control for navigation of the inverse pendulum type self-contained mobile robot", Robotics and autonomous systems, 17, pp.65-80, 1996.
[4] Baloh, M. and Parent, M.,"Modeling and Model Verification of an intelligent self-balancing two-wheeled vehicle for an autonomous urban transportation system". Conf. Comp. Intelligence, Robotic and Autonomous systems, Singapore, Dec, 15, 2003.
[5] Grasser, F., D'Arrigo, A., Comlombi, S., and Rufer, A.,"Joe: A mobile inverted pendulum", IEEE Trans. Electronics, vol. 49, no 1, pp. 107, no. 114, 2002.
[6] Kim, Y.H., Kim, S.H., and Kwak, Y.K. "Dynamic Analysis of a Nonholonomic Two-wheeled Inverted Pendulum Robot", Proc. of the Eighth Int. Symp. on Artificial Life and Robotics(AROB8th, '03), P.415-418, Beppu, Oita, Japan, 24-26 January, 2003.
[7] Nise, N.S.,"Control System Engineering, 3rd ed.", John Wiley and Son, US, 2000.
[8] Ahmad, M.N, Nawawi, S.W., Osman, J.H.S., "A full Order Sliding Mode Tracking Controller for A class of Uncertain Dynamical System", proc. ICCAS, Bangkok Thailand, pp.1853-1858, August 2004.
[9] Nawawi, S.W., Osman, J.H.S, Ahmad, M.N.,"A PI Sliding Mode Tracking Controller with Application to a 3-DOF Direct drive Robot Manipulator", TENCON2004, Vol 4, pp455-458, 2004, Thailand.

[10] Sam, M.Y., Osman, J.H.S., Ghani, R.A., "Proportional integral sliding mode control of a quarter car active suspension", TENCON02, Vol. 3, Oct 2002, pp 1630 – 1633, Beijing.

Appendices

$$A_{24} = \frac{\left(m_s d^2 + I_3\right)\tan\phi\,\dot{\psi}}{\left(m_s d\cos\phi - \dfrac{3(m_s d^2 + I_3)(m_c + m_s)}{m_s d\cos\phi}\right)}$$

$$A_{26} = \frac{\left(m_s d^2 + I_3\right)\tan\phi\,\dot{\phi}}{\left(m_s d\cos\phi - \dfrac{3(m_s d^2 + I_3)(m_c + m_s)}{m_s d\cos\phi}\right)}$$

$$A_{44} = \frac{m_s d\sin\phi\,\dot{\psi}}{m_s{}^2 d^2\cos^2\phi - 3(m_s d^2 + I_3)(m_c + m_s)}$$

$$B_{21} = B_{22} = \frac{1}{\left(m_s d\cos\phi - \dfrac{3(m_s d^2 + I_3)(m_c + m_s)}{m_s d\cos\phi}\right)} + \frac{m_s d^2 + I_3}{(Rm_s d\cos\phi)\left(m_s d\cos\phi - \dfrac{3(m_s d^2 + I_3)(m_c + m_s)}{m_s d\cos\phi}\right)}$$

$$A_{46} = \frac{m_s{}^2 d^2\cos\phi\sin\phi\,\dot{\phi} - 3(m_c + m_s)m_s d^2\sin\phi\cos\phi\,\dot{\phi}}{m_s{}^2 d^2\cos^2\phi - 3(m_s d^2 + I_3)(m_c + m_s)}$$

$$A_{66} = B_{41} = B_{42} = \frac{-m_s d^2\sin\phi\cos\phi\,\dot{(\phi)}\,3(m_c + m_s)}{(3L^2 + \frac{1}{2R^2})m_c\cos^2\phi - 3(m_c + m_s)(m_s d^2 + I_3)}$$

$$B_{61} = -B_{62} = \frac{L}{R\left[(3L^2 + \dfrac{1}{2R^2})m_c + m_s d^2\sin^2\phi + I_2\right]}$$

$$F_2 = \frac{-m_s{}^2 g d^2\sin\phi\cos\phi}{m_s{}^2 d^2\cos^2\phi - 3(m_s d^2 + I_3)(m_c + m_s)}$$

$$F_4 = \frac{-3(m_c + m_s)(m_s g d\sin\phi)}{m_s{}^2 d^2\cos^2\phi - 3(m_s d^2 + I_3)(m_c + m_s)}$$

$$A_{23} = \frac{\left(-m_s g d\right)}{m_s d - \dfrac{3(m_s d^2 + I_3)(m_c + m_s)}{m_s d}}$$

$$A_{43} = \frac{-m_s g d}{\left[\dfrac{m_s{}^2 d^2}{3(m_c + m_s)} - (m_s d^2 + I_3)\right]}$$

$$B_{21} = B_{22} = \frac{\left(m_s d^2 + I_3\right) + Rm_s d}{R\left(m_s{}^2 d^2 - 3\left(m_s d^2 + I_3\right)\left(m_c + m_s\right)\right)}$$